2017

Photoelectrochemical cell constructed from BBY membrane with various substrate materials

Yang Liu
Virginia Community Colleges

Photoelectrochemical cell constructed from BBY membrane with various substrate materials

by

Yang Liu, Master of Science in Chemical and Life Science Engineering, Virginia Commonwealth University, July 27, 2017

A thesis submitted in partial fulfillment of the requirements for the degree of Master of Science at the Virginia Commonwealth University.

Committee Members:

Dr. Stephen Fong, Associate Professor, Department of Chemical and Life Science Engineering, Virginia Commonwealth University (Committee Chair)

Dr. Nastassja Lewinski, Assistant Professor, Department of Chemical and Life Science Engineering, Virginia Commonwealth University

Dr. David Jenson, Assistant Professor, Department of Chemistry, Virginia Commonwealth University

Virginia Commonwealth University

Richmond, Virginia

July, 2017

Acknowledgement

I would like to express the appreciation to the EC Squared for their financial support.

I also want to gratefully acknowledge John Daye for his help and support on this project.

I would like to extend my gratitude to the help from Virginia Commonwealth University undergraduate students: Caleb Donkoh-Moore, Samuel Adu-Gyamfi, Maria Lopez Del Pino and Sydney Kelly.

I would like to thank Muslum Demir, Dylan Rodene, and Ramendra Pal for helping me with potentiostat usage.

I would also thank to my other lab members Qiang Yan and Eunsoo Hong for their support during my study.

Finally, I want to give special thanks to my committee members Dr. Stephen Fong, Dr. Nastassja Lewinski, and Dr. David Jenson for their contribution and advice.

Table of Contents

List of Tables

List of Figures

Abstract

PHOTOELECTROCHEMICAL CELL CONSTRUCTED FROM THYLAKOID OR BBY MEMBRANE WITH VARIOUS SUBSTRATE MATERIALS

By Yang Liu, M.S.

A thesis submitted in partial fulfillment of the requirements for the degree of Master o f Science at Virginia Commonwealth University.

Virginia Commonwealth University, 2017

Major Director: Dr. Stephen Fong, Associate Professor, Department of Chemical and Life Science Engineering.

Photoelectrochemical cells have been intensively studied in recent years with regard to using thylakoid and photosynthesis system I/II. BBY membrane is another protein complex that has potential to be utilized to build photoelectrochemical cells. Within the BBY membrane lies the highly active photosynthesis system II complex, which upon light activation, generates electrons transported within the electron transport chain during photosynthesis in green plants. This study presents an approach of immobilizing thylakoid or BBY membrane onto gold nanoparticle modified gold plate or multi-walled carbon nanotube (MWCNT) modified indium tin oxide

(ITO) coated glass substrate. The results show that BBY membrane has higher activity with a value of 168 ± 12 μmol DCIP/(mg Chl*hr) than the thylakoid, which has an activity of 67 ± 7 μmol DCIP/(mg Chl*hr). Further amperometric tests also show that BBY membrane generates a higher current than the thylakoid. We used gold based materials to build the cell first since gold has high electrical conductivity. However, in order to minimize the construction cost of cells, relatively cheap materials such as ITO coated glass and MWCNT were used instead. The surface morphology of cells was characterized using atomic force microscope (AFM) throughout cell modification. When comparing to the cell with gold material, the cell constructed with ITO and MWCNT generated a higher current density. The highest current density was found as 20.44 ± 1.58 $\mu A/cm^2$ with a system of ITO/MWCNT/BBY. More, the stability of the system was examined and the result shows a decreasing rate of 0.78 %/hour.

Chapter 1 Introduction

1.1 Background and Statement of Problems

Environmental concerns related to the consumption of carbon based energy sources, such as coal, oil, and natural gas, has risen recently and there is a demand of using alternative energy sources to replace the traditional fossil energy sources. Along rapid growth of the global economy, energy demand increases dramatically and this trend is likely to keep increasing in the future [1]. As reported by the Intergovernmental Panel on Climate Change (IPCC) in 2008, non-renewable energy supplied 85.1 % global energy consumption [2]. Associate with the non-renewable fossil energy consumption is the emission of greenhouse gases such as nitrogen oxides (NOx), carbon dioxide (CO_2), and sulfur oxides (SOx) [3]. One of the solution to alleviate the confliction between energy usage and environmental issues is replacing fossil based energy sources with renewable energy sources.

Solar energy, the radiant energy emitted from the Sun, is one of the largest available clean energy sources [4]. About 4.3 x10^{20} J solar energy arrives at surface of the Earth every hour, which is higher than the energy consumption on the planet every year (4.1 x 10^{20} J) [5]. Both passive and active technologies are applied to capture solar energy and convert it into useful energy forms, such as electrical energy and thermal energy. Although solar energy system only accounts for 1 % of all electricity produced worldwide [6], the Energy Information Administration of the United States (U.S. EIA) projected an increase of solar energy development from now on [7].

Photosynthesis is a process which converts light energy into chemical energy [8]. Most of plants perform photosynthesis to store light energy by producing glucose from carbon dioxide and water. Glucose can be then used in cellular respiration to be converted into pyruvate and release adenosine triphosphate (ATP) [9]. Two major photosynthesis apparatus, which are photosynthesis system I (PSI) and photosynthesis system II (PSII), are found to be included in the photosynthesis reaction [10]. For eukaryotes, the thylakoid disks are located within the chloroplast. In prokaryotes, the thylakoid disks are embedded in the cell membrane [11]. In this study, we focused on eukaryotes system as we extracted protein complexes from spinach leaves.

Electron transport chain (ETC) is a pathway that electrons flow within the photosynthesis system. Photons are absorbed by P680, which is the PSII primary donor, and electrons are excited to a higher energy level and then captured by plastoquinone molecules within the PSII [12]. Water acts as the electron donor in nature that bounded to the magnesium site of PSII and restored the function of P680. At the same time, water is split to produce oxygen and hydrogen ions. Plastoquinone molecules are then form plastoquinone A (Q_A), which embedds within the PSII complexes. Afterwards, electrons in the Q_A are passed further to the plastoquinone B (Q_B), which can be easily detached from the PSII and finally reaches cytochrome b6f complex where plastoquinone is reduced to plastocyanin [13]. Additionally, cytochrome b6f also transports 8 to 12 protons per 4 electrons from the stroma site to the lumen site [14]. Afterwards, plastocyanin arrives at P700, which is also excited by photons, within the PSI. Exited electrons are then transported to quinone within PSI and carried to the ferredoxin, which is outside of PSI. Finally, electrons are accepted by NADP+, which is reduced to NADPH with the presence of $NADP^+$ reductase and a pronton [15]. The exited P700 is back to ground level by accepting electrons from plastocyanin. Finally,

the generated NADPH is used in the Calvin cycle. BBY membrane , which can be extracted via the method developed by Berthold, Babcock, and Yocum [16], is obtained from the thylakoid disks and contains mainly PSII.

1.2 Specific Aims

The overall goal of this study is to test the feasibility of utilizing BBY membrane to construct a relatively cheap photoelectrochemical cell with a comparable high current density. The specific aims of this study are to:

1. **Develop a method to extract active protein complexes.** Based on literature methods, we will modify and develop the extracting method based on the instruments and chemicals we have. Additionally, the concentration and the absorption spectrum of protein complexes will be measured. The DCIP activity test will be conducted to characterize the quality of protein complexes. It is important to ensure the consistence of protein complexes supply first.

2. **Prepare linkers and develop methods to immobilize linkers onto the slides.** Two different linkers and substrates will be utilized. The first designed system will use gold material, which requires to prepare modified gold nanoparticles. Characterization of gold nanoparticles was conducted with a dynamic light scattering test and an absorption spectrum measurement. Synthesized gold nanoparticles will be then deposited onto the gold coated glass substrate to construct the first system. With consideration of the cost of the photoelectrochemical cell, indium tin oxide coated (ITO) glass substrate and multi-walled nanotubes (MWCNT) were used to construct the second system. After developing

and refining the method to suspend the MWCNT in the solvent, MWCNT will be deposited onto the ITO slide to construct the second system.

3. Characterize the constructed systems. After immobilizing protein complexes onto two systems, the current density and stability measurement were conducted. Also, atomic force microscope was used to characterize the surface topography change during system construction process. Finally, we will compare our systems with literatures with respect to the current density and stability data.

Chapter 2 Literature Review

The photoelectrochemical cell, which is constructed from photosynthesis systems, is intensively studied by researchers [17-22]. Yehezkeli group [17] immobilized PSII complex onto gold nanoparticles (AuNP), which were deposited on the gold coated glass electrode. A current of 2.7 $\mu A/cm^2$ was generated with 0.2 V applied potential and a light intensity of 0.10 W at a wavelength greater than 400 nm. Yehezkeli group [18] also constructed an electrode with PSI and PSII stacked together. The current generation was observed with a value of 2.2 $\mu A/cm^2$ under light exposure with an applied potential of 0.0 V. A higher current generation was observed when only PSI was immobilized onto the substrate with a value of 28 $\mu A/cm^2$ [23]. When only PSI was used to build the cell, a mediator was required to donate electrons to the P700 which was embedded in the PSI protein complex. A mediator can be also applied in the PSII cell system and a higher current was expected. The effects of different types of mediators to the current generation in a PSII cell system were studied by Kato, et. al. and the highest current value was 22 $\mu A/cm^2$ with 2,6-dichloro-1,4-benzoquinone (DCBQ) as the mediator [20]. Since obtaining pure and condensed PSI and PSII

proteins is a time-consuming and complex process, the thylakoid is also considered to build the photoelectrochemical cell [24]. A relatively high current was produced by Calkins, et. al. using thylakoid with a value of 68 μA/cm^2 when ferricyanide was used as a mediator [25]. Others [21, 24] observed a lower current generation after adding ferricyanide as the mediator with a range from 0.23 to 1.1 μA/cm^2 compared with the current generated by PSI and PSII fabricated cells.

Chapter 3 Protein Extraction and Gold Nanoparticle Synthesis

3.1 Thylakoid and BBY membrane extraction

Thylakoid and BBY membrane were prepared from spinach based on a previously described method with modification [26]. Briefly, 100 g spinach leaves were mixed with 300 ml BBY-1 solution (50 mM HEPES–NaOH, pH 7.5, 0.4 M NaCl, 0.2 mg/ml Bovine Serum Albumin (BSA), 2 mM MgCl2, 1mM EGTA) in a blender. Mixed solution was filtered through cheese cloth and centrifuged for 10 min at 6,000 x g and 4 °C. Then, the precipitate was resuspended in 80 ml BBY-1 solution and centrifuged for 30 s at 400 x g and 4 °C. Afterwards, precipitate was resuspended and centrifuged at 35,000 x g and 4 °C for 7 min. At this point, the obtained precipitate was suspended in 40 ml BBY-2 solution (20 mM MES–NaOH, pH 6.0, 0.15 M NaCl, 0.2 mg/ml BSA, 4 mM $MgCl_2$) and centrifuged at 35,000 x g and 4 °C for 7 min. The collected precipitate, which was the thylakoid, was suspended in 7 ml BBY-3 solution (50 mM MES–NaOH, pH 6.0, 0.4 M sucrose, 15 mM NaCl, 5 mM $MgCl_2$). 1ml of thylakoid was stored at -80 °C. To prepare the BBY membrane, 3 ml BBY-3T solution (25% (w/v) Triton X-100 in BBY-3 solution) was added into the solution slowly with stirring for 10 min. Later, the suspension was centrifuged for 15 min at 35,000 x g and 4 °C. The precipitate was resuspended in 40 ml BBY-3 solution and centrifuged

for 3 min at 3,000 x g and 4 °C. The resulting supernatant was centrifuged at 35,000 x g and 4 °C for 20 min and the precipitate, which was the BBY-membrane, was resuspended in 10 ml BBY-4 solution (50 mM MES–NaOH, pH 6.0, 0.4 M sucrose, 15 mM NaCl, 5 mM $MgCl_2$, 30% (v/v) glycerol). BBY membrane was then stored at -80 °C.

During developing the method of extracting thylakoid and BBY membrane, we experienced several obstacles. Dr. Jenson helped us to form the very first preparation method. However, at that point, we do not have the access to an ultracentrifuge as well as the homogenizer. We tried to use replace the required high speed centrifugation of 35, 000 xg with a low speed centrifugation for a longer time (up to 4 hours). However, this did not work out for us and all the proteins were still suspended in the solution. At the same time, we did not have a homogenizer to mix our samples. Therefore, we tried both vortex mixer and sonicating mixing. As result, the concentration of the protein we got was very low when compared to using homogenizing mixer (Supplementary 6).

The chlorophyll concentration of both thylakoid and BBY membrane were measured by UV-Vis (BioMate 3) at a wavelength of 645 nm, 663 nm, and 720 nm [26]. The concentration was calculated via Equation 1 based on the absorbance measured by the UV-Vis. The activity of thylakoid and BBY membrane were characterized with dichlorophenolindophenol (DCIP) [27, 28]. During exposure to light, thylakoid and BBY membrane produced electrons and transport electrons through the electron transport chain. Finally, the DCIP was reduced after receiving electrons from the protein complex. The change of solution absorbance at 600 nm before and after light exposure

was used to calculate the activity of protein complex with respect to the DCIP concentration. The calibration curve of DCIP concentration was shown in supplementary 1.

$$Total\ Chlorophyll = \frac{8.05 \times (A_{663} - A_{720}) + 20.29 \times (A_{645} - A_{720})}{DF} \qquad \text{Equation 1}$$

Where,

A_{663}: Absorbance measured at 663 nm.

A_{645}: Absorbance measured at 645 nm.

A_{720}: Absorbance measured at 720 nm.

DF: Dilution factor

When testing the activity of proteins, we also solved several challenges and finally formed the working protocols. At the first place, we tried to use the oxygen assay to determine the activity of obtained proteins. Oxygen calibration was performed by two-point calibration method. Oxygen probe was submerged into a zero oxygen standard solution to calibrate the 0.00 % oxygen point. Then, oxygen probe was exposed to ambient air which contains 20.96% oxygen to calibrate the 100.00 % oxygen point. However, the calibration of the probe failed since it did not meet the instrumental requirement. According to the manual, the probe needed to be replaced. But we still used the probe for the following oxygen assay. The calibration curve and detailed experimental data was shown in supplementary 7. Since we do not have the access to a proper working oxygen probe, we tried to build the probe by ourselves (supplementary 8). A platinum disk and a Ag/AgCl electrode was used and immersed into the diluted samples. Both pure oxygen and nitrogen were

used to calibrate the oxygen probe before each experimental run. During testing, 10 μg/ml protein samples were used and a total volume of 10 ml was used. The results showed that the oxygen activity of BBY membrane was 308.18 ± 11.92 umol O_2/mg Chl/hr. Moreover, along with the preparation of the protein complexes, we found that the pH of the buffer solution was importatnt. Previously, we failed to pay attention on the pH value of the buffer solution we prepared. Later, we found a very low value of protein activity or no activity at all. Finally, we identified that the pH of some buffer solution was very low with a value of 2 to 3. After adjusted the pH to the idea range, the protein samples we got showed a comparable activity value.

Futhermore, in order to determine the the composition of the extracted protein complexes, protein gel (12% Mini-PROTEAN® TGX™ Gel, 10 well, 30 μl) was used to identify the proteins. The results were shown in supplementary 9. Four major bands were identified which supported the presence of PSII. The absorption spectrum of both thylakoid and BBY membrane was listed in supplementary 3, which shown a major absorption peak at around 438 nm and 680 nm.

3.2 Gold nanoparticle synthesis and modification

Modified gold nanoparticles were synthesized based on a previously described process [29] with a black color (supplementary 4). Electropolymerization was conducted to deposit gold nanoparticles onto the modified gold slide surface. During the process, 6 cycles between -1.2 to 0.4 V at a scan rate of 0.05 V/s were applied. The cyclic voltammogram was shown in supplementary 5. The final concentration of AuNP was calculated based on the concentration of chloroauric acid used during synthesis process. The hydrodynamic diameter of AuNP was

measured by the dynamic light scattering (DLS) (Malvern Zetasizer Nano-ZS). Prior to measurement, AuNP suspended solution was filtered through a 4 μm disk filter. Also, the spectrum of the AuNP was measured by the UV-Vis.

Prior to synthesis and modify the gold nanoparticle, unmodified gold nanoparticles were synthesized based on the Turkevich method [30]. 20 ml of 1.0 mM $HAuCl_4$ solution was added to a 50 ml Erlenmeyer flask. The solution was heated to boil with a stirring. Then, 2 ml of a 1 % solution of trisodium citrate dehydrate was quickly added into the solution. After 10 minutes of reaction, the flask was removed from the heat and gold nanoparticles was synthesized in the solution. Samples were filtered through a 0.4 μm filter disk to remove dust particles. DLS was used to determine the size of the AuNPs. The size of the AuNPs was 19.62 ± 2.99 nm. The final concentration of the solution is 180 ug/ml. In addition, UV-Vis was used to confirm that Au NPs was successfully synthesized. The UV-Vis results of synthesized AuNPs were shown in supplementary 10.

3.3 Results and Discussion

The chlorophyll concentration of both thylakoid and BBY membrane were measured as 6.10 ± 0.03 mg/ml and 3.44 ± 0.03 mg/ml based on at least three samples, respectively. The protein activity was tested with DCIP and the result shows that thylakoid had an activity of 67 ± 7 μmol DCIP/(mg Chl*hr) (Table 1). For reference, thylakoid activity was previously measured by Romanowska et. al. group to be 68 ± 8 μmol DCIP/(mg Chl*hr) and this value was comparable with our result [28]. The activity of BBY membrane was quantified as 168 ± 12 μmol DCIP/(mg

Chl*hr), which was similar to the activity value of 167 µmol DCIP/(mg Chl*hr) determined by Shen et. al. group [27].

Table 1. Activity of both thylakoid and BBY membrane. Electrons generated during light exposure from the protein complex were accepted by the DCIP.

Protein Complex	Activity (µmol DCIP/(mg Chl*hr))
Thylakoid (This Study)	67 ± 7
Thylakoid **[28]**	68 ± 8
BBY Membrane (This Study)	168 ± 12
BBY Membrane **[27]**	167

The concentration of the AuNP was calculated as 11.4 mg/ml and the hydrodynamic size of AuNP was measured as 5.713 ± 0.172 nm. Different size of AuNP could be obtained by using different concentration of reducing agent and different types of reducing agent [30]. The absorption spectrum of AuNP was shown in Figure 1.

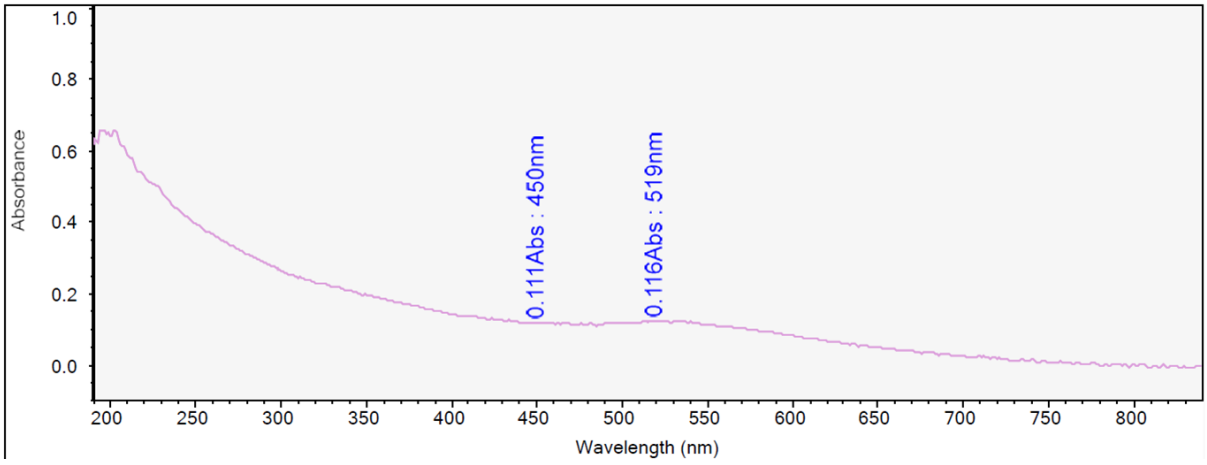

Figure 1. Absorption spectrum of AuNP.

Chapter 4 The Au/AuNP/Protein System and the ITO/MWCNT/Protein System

4.1 Photoelectrochemical cell construction

Both gold coated glass substrate (LGA Thin Films, 100 nm Au over 10 nm Ti adhesion layer) and ITO coated glass substrate (Delta Technologies, LTD, R_S = 4 - 8 Ω/sq, Coating Thickness 1,500 - 2,000 Å) were washed by soap water, deionized water, acetone (ACS grade, >99.5 %), and ethanol (ACS grade, >99.5 %) for 10 min each in an ultrasonic bath (Fisher Scientific, FS30H). The gold slide was then immersed into a 10 mM p-aminothiophenol solution (in ethanol) for 5 hours at room temperature, then washed with a 0.1 M phosphate buffer (pH 7.5 and filtered through a 0.4 um filter disk).

10 μl of thylakoid or BBY membrane with a diluted chlorophyll concentration of 1 mg/ml was immobilized onto the gold nanoparticle modified substrate surface, which has an area of 0.02 cm^2, via dropcasting method. In the end, the slide was rinsed with 2 ml BBY-4 solution to get rid of any unbound protein complexes. The construction that used gold nanoparticle modified gold coated glass as substrate and immobilized thylakoid or BBY membrane onto the slide is abbreviated as Au/AuNP/Thylakoid and Au/AuNP/BBY. The structure diagram was shown in Figure 2.

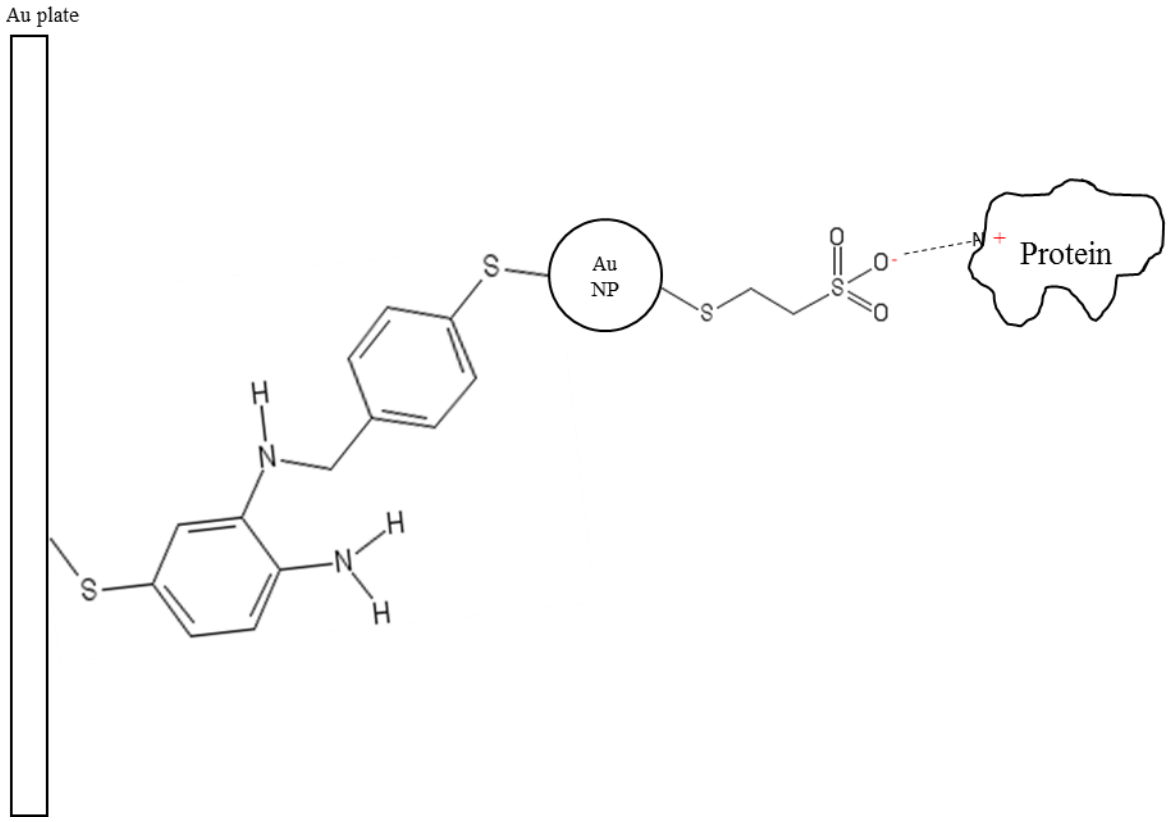

Figure 2. Structure diagram of Au/AuNP/protein. Only one AuNP/protein attachment to the substrate was shown.

The MWCNT (length 10-30 μm, outer diameter 8 nm, inner diameter 2-5 nm, purity >95 %) was dispersed in the dimethylformamide (DMF) solution (sequencing grade, ≥99.5 %) at a concentration of 6 mg/ml with the assistance of ultrasonic probe (Cole Parmer, CV33) for 10 min. Then, the solution was transferred into a test tube and immersed into the ultrasonic bath for 1 hour. The dispersed MWCNT suspension of 4 μl was immobilized onto the ITO slide with an area of 0.02 cm^2. The slide was dried at 70 °C overnight. On the next day, 4 μL 1-Pyrenebutyric acid N-hydroxysuccinimide ester (PBSE) with a concentration of 10 μM was added to the substrate surface. After 45 min incubation on ice, unbounded PBSE was rinsed off with DMF and the surface

was neutralized with the BBY-4 solution. Next, 14 μg of thylakoid or BBY membrane was immobilized onto the MWCNT modified ITO slide by dropcasting. Finally, the cell was washed with the BBY-4 solution to remove unbound protein complexes. The construction that used MWCNT modified ITO coated glass as substrate and immobilized thylakoid or BBY membrane onto the cell is abbreviated as ITO/MWCNT/Thylakoid and ITO/MWCNT/BBY. The structure diagram was shown in Figure 3. The picture of the final constructed photoelectrochemical cell could be found in supplementary 2.

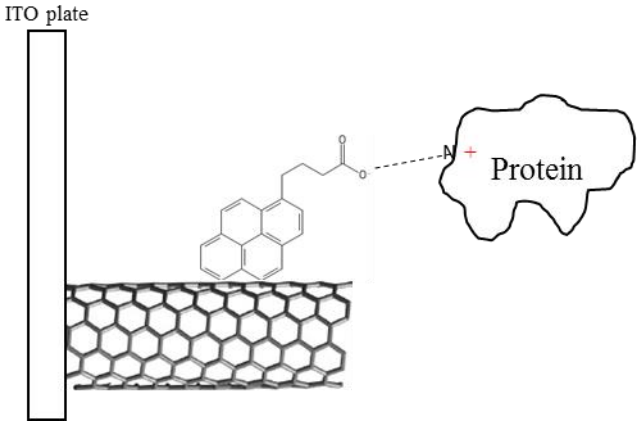

Figure 3. Structure diagram of ITO/MWCNT/protein. Only one MWCNT/protein attachment to the substrate was shown.

A potentiostat (CH Instruments, CHI600E) was used to measure the current generation of photoelectrochemical cells. The amperometric i-t method was used with a potential of 0.2 V. 1.5 mM potassium ferricyanide was used as the electron mediator and 0.1 M phosphate buffer was used as the electrolyte solution. A fiber optic illuminator (Fiber-Lite, Model 190) was used as the light source with a light intensity of 2.37 mW/cm^2 at 635 nm, which was measured by a photodiode power sensor (Thorlabs PM200) with a sensor head (Thorlabs S310C). During the

photoelectrochemical measurements, a KCl saturated Ag/AgCl electrode and a platinum electrode were used as the reference electrode and counter electrode, respectively.

In order to understand the change of the surface morphology throughout surface modification, atomic force microscope (AFM) (VEECO ICON) was used to detect the surface roughness of cells. During the examination, tapping mode and a probe with aluminum coating (Bruker AFM Probes, TESPA) was used. AFM images of pristine gold plate, gold nanoparticles modified gold slide, pristine ITO plate, MWCNT modified ITO slide, thylakoid immobilized cell, and BBY membrane immobilized cell were obtained.

Moreover, another proposed approach to immobilize the AuNPs onto the Au slide was considered (supplementary 11). Since the concentration of proteins, which actually attached onto the slides, were relatively low, this method was not continued and therefore modified AuNPs were used instead of using non-modifield AuNPs.

We also considered to to use a homebuild system to measure the current density of the constructed photoelectrochemical cell. The scheme of the build was shown in supplementary 12. Since we do not have the access to all of the instruments and the potentiostat was easy to use so for measuring the current density, we finally did not went to contruct the measuring platform.

In addition, the scanning electron microscope (SEM) (JEOL JSM-5610LV) was used to visually identify the deposition of AuNPs, MWCNT, and the protein complexes. The images were shown in supplementary 13. However, we were not able to capture a good quality of images because it reached the instrument limitation.

At the first place, we tried to disperse MWCNT into water or DMF with the assistance of sonification bath. TX-100 was also added in the suspension to help the dispersion. However, when we conducting the electrodeposition of MWCNT, the ITO was washed off from the glass slide. Therefore, no surfactant agents were used in the later experiements. Another solution we found was to modify the surface of the MWCNT with carboxylic acid group. MWCNT surface was modified by mixing 0.03 g MWCNT with 25 ml concentrated HNO_3 (15.6 M) and heated to 80 °C. Consequently, MWCNT surface was functionalized with carboxylic acid group which created a more hydrophilic surface structure. Then, functionalized MWCNT was washed with DI water until the pH of effluent reached neutral. Finally, functionalized MWCNT was dried in the air. About 47 wt.% of MWCNT was lost during the process. Functionalized MWCNT was added into 100 ml DI water and sonicated for 3 hours in a sonicator bath. Part of the MWCNT was well dispersed in the solution. Although we had some dispersion of MWCNT, the whole process is complicated and time consuming. Later, we found a stronger ultrasonicating probe which helped to disperse the MWCNT into the solution perfectly. With respect to the deposition of MWCNT, we tried the electrodeposition. The ITO surface was hydrolyzed first with hydrogen peroxide and used as the cathode. A platinum wire was also used as an anode. The distance of two electrodes was 1 cm. Before electrodeposition, 0.1M $Mg(NO_3)_2 \cdot 6H_2O$ was added into the CNT solution to give the MWCNT a positive charge. 30 V power source was used and the experiment ran for 60s. After

electrodeposition, an uneven surface was observed. Then, we changed the platinum wire with a flat copper to be used as the anode. Finally, we got a even distributed surface. After electrodeoposition, the slide was dried at 70 °C overnight. Figures of the electrodeposition was listed in supplementary 14.

We also troubleshooted the current density measurements. At first place, we experienced a delay of the current signal when we turned on/off the light (supplementary 15). We found out that the effective area of the slide would affect the delay. When we used a large area (1 cm^2), there was an obvious delay. When we reduced the effect area to 0.02 cm^2, no delay was observed at all. One of the possible reason was that our light source is a point light source. For a large area, it woud not receive the same amount of photons at different locations which could possibly casuing a signal delay. When we got the first no delayed signal, we observed a instantaneous increase of the current. Since the current change was small, a statistical test was applied to determine if it was a significant change. The results showed that there was a significant change with a p value of 2.15×10^{-6}.

4.2 Results and Discussion

Figure 4 (a) depicts one of the light on and off tests of the Au/AuNP/Thylakoid system. An immediate current change was observed when the light was turned on and off. The average current density produced by this system was measured as 0.90 ± 0.04 $\mu A/cm^2$. Figure 4 (b) shows one of the light on and off tests of the Au/AuNP/BBY system. The average current density produced by this system was slightly higher with a value of 1.00 ± 0.12 $\mu A/cm^2$. 0.15 M potassium ferricyanide was used as the mediator.

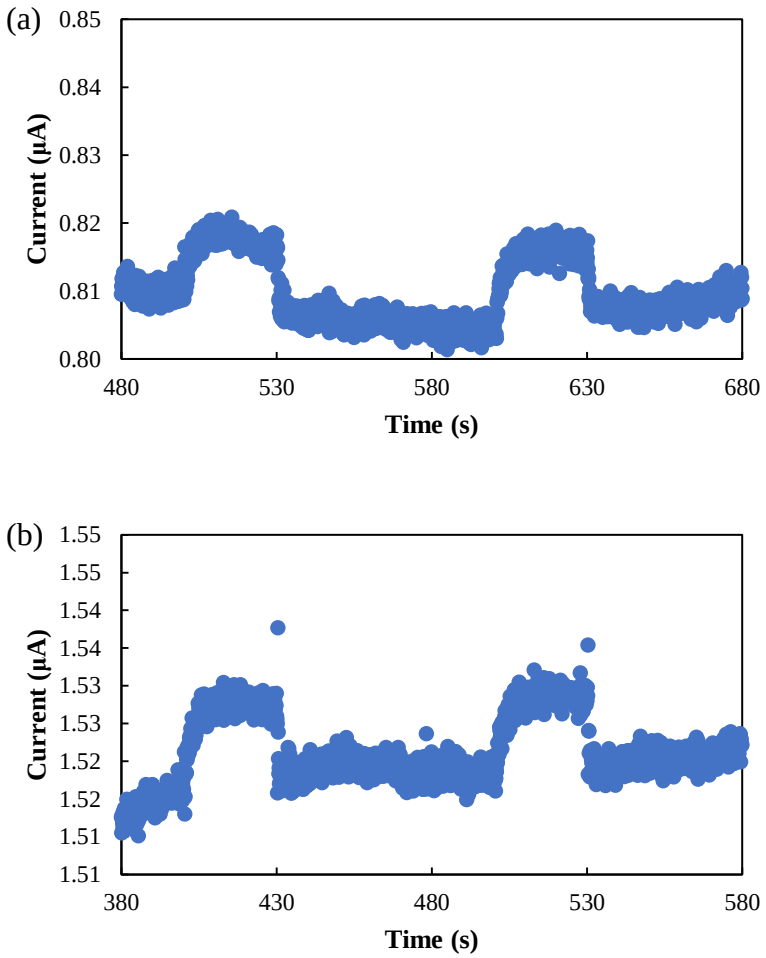

Figure 4. (a) Au/AuNP/Thylakoid system. The light was turned on at both 500 and 600 s for 30 s. (b) Au/AuNP/BBY system. The light was turned on at both 400 and 500 s for 30 s.

Figure 5 (a) shows a repeated light on and off test of the ITO/MWCNT/Thylakoid system. The average current density was measured as 12.51 ± 0.98 μA/cm^2. The current produced by the photoelectrochemical cell decreased as the light on and off cycle increased. Figure 5 (b) shows multiple cycles of light on and off test. The ITO/MWCNT/BBY system produced a higher average current density of 20.44 ± 1.58 μA/cm^2.

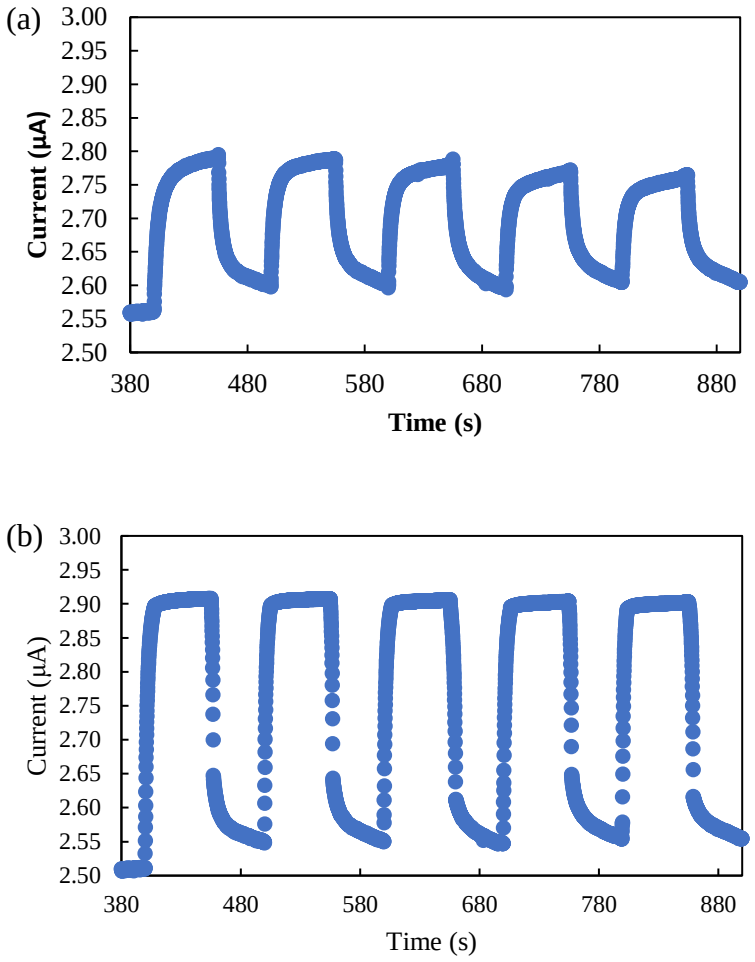

Figure 5. (a) ITO/MWCNT/Thylakoid system. The light was turned on at 400, 500, 600, 700 and 800 s for 55 s. (b) ITO/MWCNT/BBY system. The light was turned on at 400, 500, 600, 700 and 800 s for 55 s.

In order to understand the current change under long-time light exposure, a stability test was conducted and the cell was exposed under light for 1220 s. The ITO/MWCNT/BBY system, which generates the highest current, was used during test. According to Figure 6, the current decreasing rate was calculated as 0.78 %/hour.

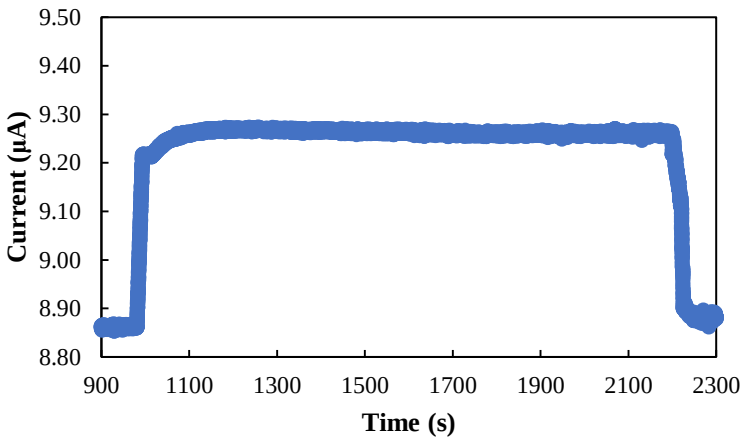

Figure 6. ITO/MWCNT/BBY system stability test. The light was turned on at 980 s for 1220 s. Cell area was 0.02 cm^2 and 0.15 M potassium ferricyanide was used as the mediator.

The AFM images of pristine gold coated glass substrate, gold nanoparticle modified slide, Au/AuNP/Thylakoid slide, and Au/AuNP/BBY cell are shown in Figure 7. After AuNP deposition, the surface roughness increased from 2.52 nm (Fig. 7 (a)) to 4.80 nm (Fig. 7 (b)) and height increased from 24.1 nm to 35.4 nm confirming successful gold nanoparticle immobilization. Furthermore, the fabrication of thylakoid and BBY membrane onto the surface increased the surface roughness to 5.00 nm (Fig. 7 (c)) and 4.84 nm (Fig. 7 (d)) and the height to 38.5 nm and 39.2 nm. Although the surface roughness only changed 0.04 nm after immobilizing the BBY membrane, the height difference after immobilizing the BBY membrane was 3.8 nm. Since the thylakoid thickness was estimated as 4 nm [31], one layer of thylakoid and BBY membrane was likely formed on the slide surface. The amount of protein complex on slides was calculated by measuring the difference between the thylakoid or BBY membrane solution concentration before immobilization and the protein concentration in the washing solution after immobilization. The

results show that 0.020 ± 0.003 mg/cm^2 of thylakoid and 0.016 ± 0.002 mg/cm^2 of BBY membrane were deposited on slides.

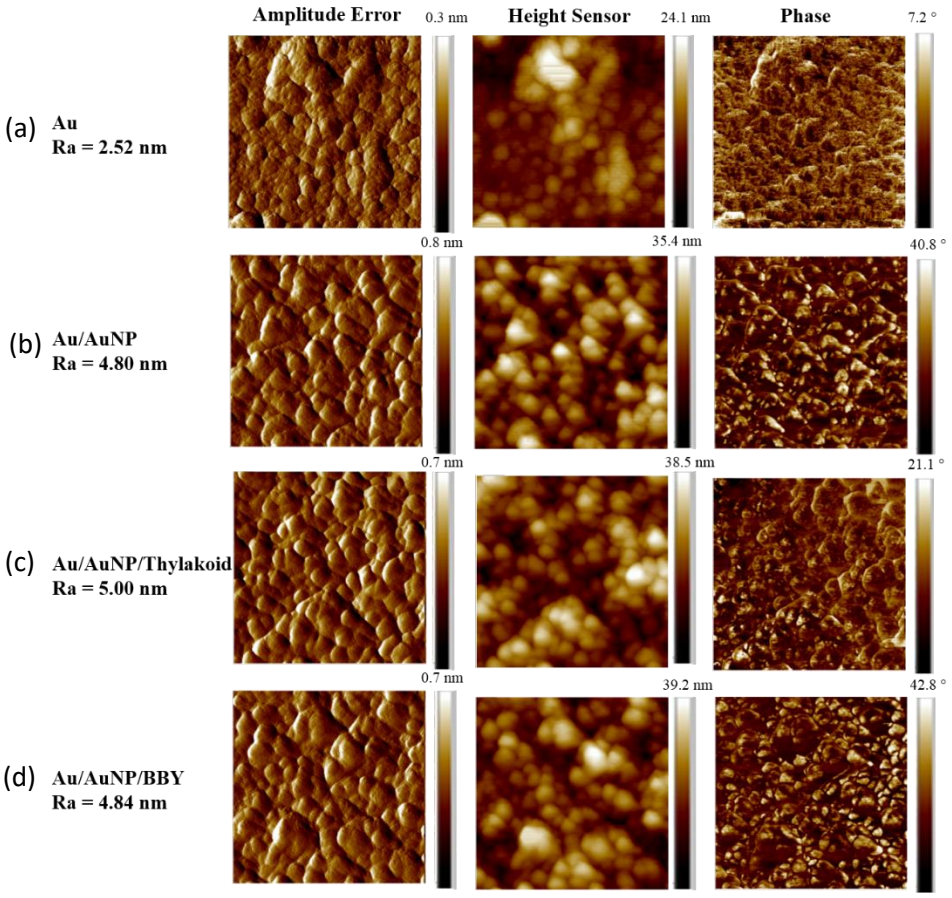

Figure 7. AFM images of (a) Au slide, (b) Au slide with Au nanoparticles, (c) Au/AuNP/BBY, and (d) Au/AuNP/Thylakoid systems. The surface roughness (Ra) increased from 2.52 nm to 4.80 nm after deposition of AuNP and increased to 5.00 nm or 4.84 nm after deposition of thylakoid or BBY membrane.

The AFM images of pristine ITO coated glass substrate (Fig. 8 (a)), MWCNT modified slide (Fig. 8 (b)), ITO/MWCNT/Thylakoid cell (Fig. 8 (c)), and ITO/MWCNT/BBY cell (Fig. 8 (d)) are shown in Figure 8. The surface roughness of pristine ITO coated glass substrate was 3.2 nm and

the height was 25.1 nm. After fabrication of MWCNT onto the substrate surface, the surface roughness increased to 27.9 nm and the height increased to 219.9 nm. Further immobilization of thylakoid and BBY membrane increased the surface roughness to 34.8 nm and 32.1 nm and the height to 272.5 nm and 243.3 nm. Additionally, concentration measurement performed before and after immobilization of thylakoid and BBY membrane confirmed the successful deposition of protein complex onto the slide surface. The results show that 0.450 ± 0.012 mg/cm^2 of thylakoid and 0.445 ± 0.028 mg/cm^2 BBY membrane were immobilized onto the electrode surface.

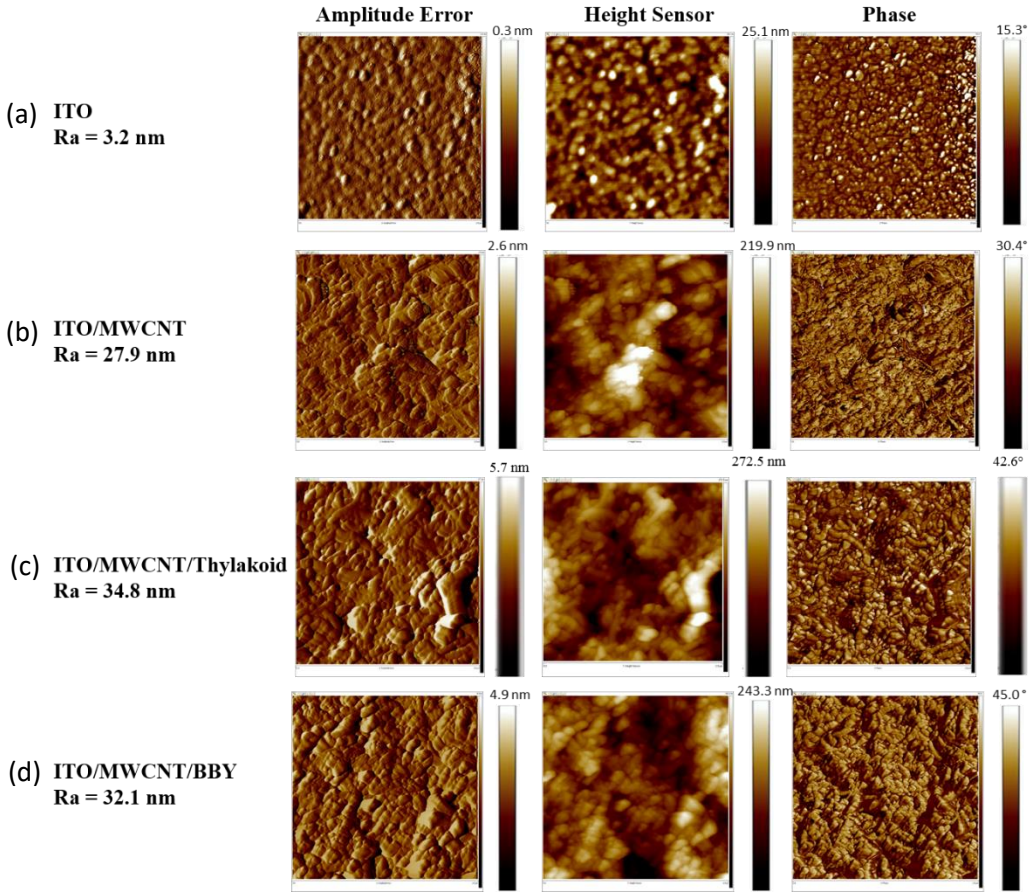

Figure 8. AFM image of ITO/MWCNT/BBY and ITO/MWCNT/Thylakoid systems. The surface roughness increased from 3.2 nm to 27.9 after the deposition of MWCNT and increased to 34.8 nm or 32.1 nm after deposition of thylakoid or BBY membrane.

The present study introduces four different systems, which include Au/AuNP/Thylakoid, Au/AuNP/BBY, ITO/MWCNT/Thylakoid, and ITO/MWCNT/BBY. Based on the results shown above, BBY membrane has higher activity and generated a higher current compared to the thylakoid. Also, cells that replaced expensive gold material with relatively cheap ITO and MWCNT generated a comparable current. Additionally, the stability result of ITO/MWCNT/BBY cell shows the system was relatively stable when compared to other literature results [17, 18, 32-34]. However, further study on improving the stability of the system is needed.

Most existing photoelectrochemical studies have focused on using thylakoid, PS I, and PS II to construct the photoelectrochemical cell [35-38]. In this study, we found that BBY membrane has several advantages for the photoelectrochemical cell construction. As mentioned before, thylakoid membrane is easier to extract and purify compared to PSI and PSII. BBY membrane, which was introduced in the 1980s, was prepared by washing the thylakoid with detergent and resulted with a PSII enriched membrane. BBY membrane is easier to obtain compared to PSI and PSII. Additionally, after testing the activity of both thylakoid and BBY membrane, the result shows that BBY membrane has a higher activity than thylakoid. Further current density measurements confirmed that BBY membrane can generate more current than thylakoid. The comparison of photocurrent density between this study and literatures were summarized in Table 2. The ITO/MWCNT/BBY system generated a comparable value of photocurrent density.

Table 2. The photocurrent density comparison between this study and selected literatures.

	Photosystem	**Photocurrent density, μA/cm²**	**Applied potential, V (vs. Ag/AgCl)**
This Study	BBY	20.44 ± 1.58	0.2
Bhalla et. al. [33]	BBY	0.16 [e]	0.62
Yehezkeli et. al. [18]	PSI	9.6 [a]	-0.05
	PSII	2	0.0
	PSI+PSII	2.2	0.0
Yehezkeli et. al. [17]	PSII	2.7	0.2
Badura et. al. [32]	PSII	45	0.3
Kato et. al. [20]	PSII	1.6, 12 [c], 22 [d]	0.5
Terasaki et. al. [36]	PSII	2.44	0.2
Yehezkeli et. al. [39]	PSI	4 [a]	0.3
Ciesielski et. al. [19]	PSI	2 [a]	0.0
Efrati et. al. [35]	PSI	2.25, 1.5	0.0
Lee et. al. [21]	Thylakoid	0.23 [b]	0.4
Calkins et. al. [25]	Thylakoid	68 [b]	0.2
Ahmed et. al. [24]	Thylakoid	1.1	5.2 μV
Lam et. al. [38]	Thylakoid	1.1 [f]	5.2 μV
Mediators: [a] Dichlorophenolindophenol (DCIP)/ascorbic acid; [b] $Fe(CN)_6^{3-/4-}$; [c] 1,4-naphthoquinone-2-sulfonate (NQS); [d] 2,5-Dichloro-1,4-benzoquinone (DCBQ); [e] Duroquinone; [f] 2-hydroxy-1,4-naphthoquinone (HNQ)			

In order to construct a photoelectrochemical cell with relatively cheap materials that can still generate a comparable current density, ITO coated glass substrate and MWCNT were considered to replace gold coated glass substrate and gold nanoparticles. As stated in the results, more protein complexes were able to immobilize onto the ITO/MWCNT slide. This could be the result of the large surface area of the MWCNT. Although gold material has a higher electrical conductivity,

higher current was generated by ITO/MWCNT slide due to a greater amount of functional protein complexes on the surface.

With a comparable current density generation and a relatively cheap cell system. One of the other concerns about the cell is the stability. The stability test of ITO/MWCNT/BBY cell was conducted with light on for 20 min. The decreasing rate of current density was relatively low when compared to literature stability tests with decreasing rates of 1.5 %/hr [17], 0.33 %/hr [18], 14 %/hr [32], 2.08 %/hr [33], and 10 %/hr [34]. However, the stability of the photoelectrochemical cell still needs to be improved so it can produce the same amount of current in a long period to compete with the traditional types of solar cell.

Chapter 5 Conclusion and Future Perspective

5.1 Conclusion

Photoelectrochemical cells made from thylakoid and BBY membrane were demonstrated in this study using both Au/AuNP and ITO/MWCNT assemblies. Compare to PSI and PSII protein complexes, BBY membrane was easier to extract and purify. Moreover, compared to thylakoid, BBY membrane had a higher activity and can generate a higher current density of 20.44 ± 1.58 $\mu A/cm^2$ with the ITO/MWCNT/BBY construction. In order to minimize the cost of construction of the photoelectrochemical cell, relatively cheaper materials of ITO coated glass substrate and MWCNT were used to replace the expensive gold material. An increased current density was observed after switching from the Au/AuNP assembly to ITO/MWCNT indicating the cheaper assembly materials would provide sufficient conductivity to complete the cell. The result of a long-

time light exposure experiment, which was conducted with the ITO/MWCNT/BBY cell, showed a decreasing rate of 0.78 %/hour. Results confirm that BBY membrane can generate a comparable amount of current to serve as a possible renewable energy source when combined with less expensive ITO/MWCNT supports.

5.2 Future Perspective

Future research could focus on two directions. First, enhancing the current density produced by the system. A direction controlled deposition of MWCNT onto the substrate may help to study the orientation effects. Also, switch the light source to a light source with a specific wavelength will help to increase the current density since the PSII in the BBY membrane absorbs light energy mostly at 680 nm. Secondly, the research on the stability or self-regeneration needs to be intensively studied. Compare to a commercial solar panel, the stability of this photoelectrochemical cell is very low. Since proteins were used in the system and the degradation of proteins is fast, mimic the self-regeneration system in the plants could be a way to solve the stability issue of the system.

References

1. Kaygusuz K, Bilgen S. Energy related environmental policies in Turkey. Energy Sources, Part B. 2008;3(4):396-410.

2. Edenhofer O, Pichs-Madruga R, Sokona Y, Seyboth K, Matschoss P, Kadner S, et al. IPCC special report on renewable energy sources and climate change mitigation. Prepared By Working Group III of the Intergovernmental Panel on Climate Change, Cambridge University Press, Cambridge, UK. 2011.

3. Quadrelli R, Peterson S. The energy–climate challenge: recent trends in CO 2 emissions from fuel combustion. Energy policy. 2007;35(11):5938-52.

4. Lewis NS, Nocera DG. Powering the planet: Chemical challenges in solar energy utilization. Proceedings of the National Academy of Sciences. 2006;103(43):15729-35.

5. Lewis NS, Crabtree G. Basic research needs for solar energy utilization: report of the basic energy sciences workshop on solar energy utilization, April 18-21, 2005. US Department of Energy, Office of Basic Energy Science; 2005.

6. Schiffer H-W, Westhuizen ZVd, Ibeanu CRN, Onyekpe DK, Notariannl E, Menzel C. World Energy Resources 2016. United Kingtom: World Energy Council, 2016.

7. Annual Energy Outlook 2017 [Internet]. U.S. Energy Information Administration; 2017. Available from: https://www.eia.gov/outlooks/aeo/

8. Rabinowitch E. Photosynthesis. Photosynthesis. 1969.

9. Hopkins WG. Photosynthesis and respiration: Infobase Publishing; 2006.

10. Renger G. Primary processes of photosynthesis: principles and apparatus: Royal Society of Chemistry; 2008.

11. Vermaas W. Revealing the secrets of old sol's sugar factories. WORLD AND I. 1998;13:158-65.

12. Metz JG, Nixon PJ, Rogner M, Brudvig GW, Diner BA. Directed alteration of the D1 polypeptide of photosystem II: evidence that tyrosine-161 is the redox component, Z, connecting the oxygen-evolving complex to the primary electron donor, P680. Biochemistry. 1989;28(17):6960-9.

13. Kurisu G, Zhang H, Smith JL, Cramer WA. Structure of the cytochrome b6f complex of oxygenic photosynthesis: tuning the cavity. Science. 2003;302(5647):1009-14.

14. Shikanai T, Munekage Y, Kimura K. Regulation of proton-to-electron stoichiometry in photosynthetic electron transport: physiological function in photoprotection. Journal of plant research. 2002;115(1):0003-10.

15. Voet D, Voet J. Biochemistry, 2nd edn., J. Wiley & Sons, New York; 1995.

16. Berthold DA, Babcock GT, Yocum CF. A highly resolved, oxygen-evolving photosystem II preparation from spinach thylakoid membranes: EPR and electron-transport properties. Febs Letters. 1981;134(2):231-4.

17. Yehezkeli O, Tel-Vered R, Wasserman J, Trifonov A, Michaeli D, Nechushtai R, et al. Integrated photosystem II-based photo-bioelectrochemical cells. Nature communications. 2012;3:742.

18. Yehezkeli O, Tel-Vered R, Michaeli D, Nechushtai R, Willner I. Photosystem I (PSI)/Photosystem II (PSII)-Based Photo-Bioelectrochemical Cells Revealing Directional Generation of Photocurrents. Small. 2013;9(17):2970-8.

19. Ciesielski PN, Hijazi FM, Scott AM, Faulkner CJ, Beard L, Emmett K, et al. Photosystem I–Based biohybrid photoelectrochemical cells. Bioresource technology. 2010;101(9):3047-53.

20. Kato M, Cardona T, Rutherford AW, Reisner E. Photoelectrochemical water oxidation with photosystem II integrated in a mesoporous indium–tin oxide electrode. Journal of the American Chemical Society. 2012;134(20):8332-5.

21. Lee J, Im J, Kim S. Mediatorless solar energy conversion by covalently bonded thylakoid monolayer on the glassy carbon electrode. Bioelectrochemistry. 2016;108:21-7.

22. Crowder E. Bio-Solar Cells. Google Patents; 2012.

23. Mershin A, Matsumoto K, Kaiser L, Yu D, Vaughn M, Nazeeruddin MK, et al. Self-assembled photosystem-I biophotovoltaics on nanostructured TiO2 and ZnO. Scientific reports. 2012;2.

24. Ahmed J, Park W, Kim S. Photoelectric activity of thylakoid layer formed on gold via aminoalkanethiol self-assembled monolayers. Bulletin of the Korean Chemical Society. 2009;30(10):2195-6.

25. Calkins JO, Umasankar Y, O'Neill H, Ramasamy RP. High photo-electrochemical activity of thylakoid–carbon nanotube composites for photosynthetic energy conversion. Energy & Environmental Science. 2013;6(6):1891-900.

26. Carpentier R. Photosynthesis research protocols: Springer; 2004.

27. Shen J-R, Terashima I, Katoh S. Cause for dark, chilling-induced inactivation of photosynthetic oxygen-evolving system in cucumber leaves. Plant Physiology. 1990;93(4):1354-7.

28. Romanowska E, Wasilewska W, Fristedt R, Vener AV, Zienkiewicz M. Phosphorylation of PSII proteins in maize thylakoids in the presence of Pb ions. Journal of plant physiology. 2012;169(4):345-52.

29. Riskin M, Tel-Vered R, Lioubashevski O, Willner I. Ultrasensitive surface plasmon resonance detection of trinitrotoluene by a bis-aniline-cross-linked Au nanoparticles composite. Journal of the American Chemical Society. 2009;131(21):7368-78.

30. Kimling J, Maier M, Okenve B, Kotaidis V, Ballot H, Plech A. Turkevich method for gold nanoparticle synthesis revisited. The Journal of Physical Chemistry B. 2006;110(32):15700-7.

31. Pribil M, Labs M, Leister D. Structure and dynamics of thylakoids in land plants. Journal of experimental botany. 2014;65(8):1955-72.

32. Badura A, Guschin D, Esper B, Kothe T, Neugebauer S, Schuhmann W, et al. Photo-induced electron transfer between photosystem 2 via cross-linked redox hydrogels. Electroanalysis. 2008;20(10):1043-7.

33. Bhalla V, Zazubovich V. Self-assembly and sensor response of photosynthetic reaction centers on screen-printed electrodes. Analytica chimica acta. 2011;707(1):184-90.

34. Ham M-H, Choi JH, Boghossian AA, Jeng ES, Graff RA, Heller DA, et al. Photoelectrochemical complexes for solar energy conversion that chemically and autonomously regenerate. Nature chemistry. 2010;2(11):929-36.

35. Efrati A, Lu C-H, Michaeli D, Nechushtai R, Alsaoub S, Schuhmann W, et al. Assembly of photo-bioelectrochemical cells using photosystem I-functionalized electrodes. Nature Energy. 2016;1:15021.

36. Terasaki N, Iwai M, Yamamoto N, Hiraga T, Yamada S, Inoue Y. Photocurrent generation properties of Histag-photosystem II immobilized on nanostructured gold electrode. Thin Solid Films. 2008;516(9):2553-7.

37. Shon Y, Kim H, Hwang HS, Bae ES, Eom T, Park EJ, et al. A nanostructured cell-free photosynthetic biocomposite via molecularly controlled layer-by-layer assembly. Sensors and Actuators B: Chemical. 2017;244:1-10.

38. Lam KB, Johnson EA, Chiao M, Lin L. A MEMS photosynthetic electrochemical cell powered by subcellular plant photosystems. Journal of Microelectromechanical Systems. 2006;15(5):1243-50.

39. Yehezkeli O, Wilner OI, Tel-Vered R, Roizman-Sade D, Nechushtai R, Willner I. Generation of photocurrents by bis-aniline-cross-linked Pt nanoparticle/photosystem I composites on electrodes. The Journal of Physical Chemistry B. 2010;114(45):14383-8.

Supplementary Information

1. DCIP calibration curve used to determine the activity of thylakoid and BBY membrane

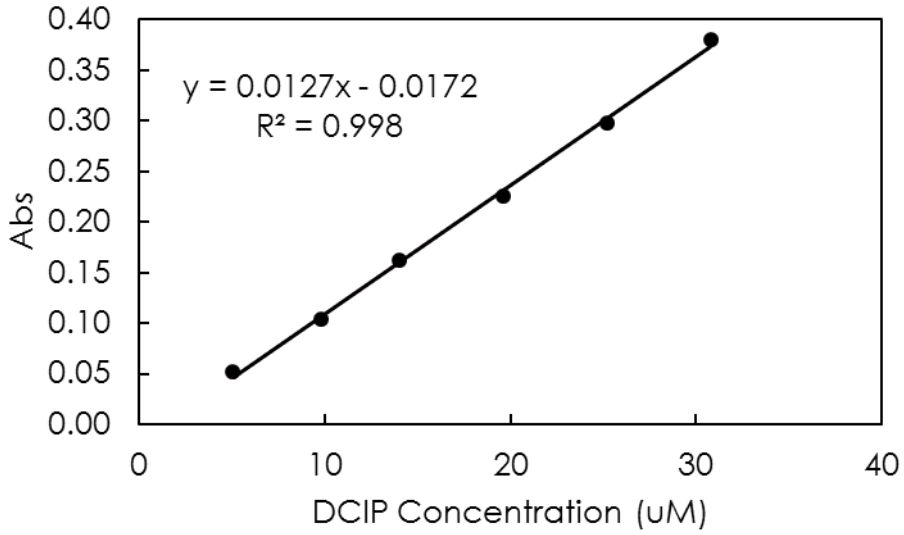

UV-Vis calibration curve of different concentration of the DCIP.

2. Image of ITO/MWCNT/BBY slide

3. UV-Vis absorption spectrum of thylakoid and BBY membrane

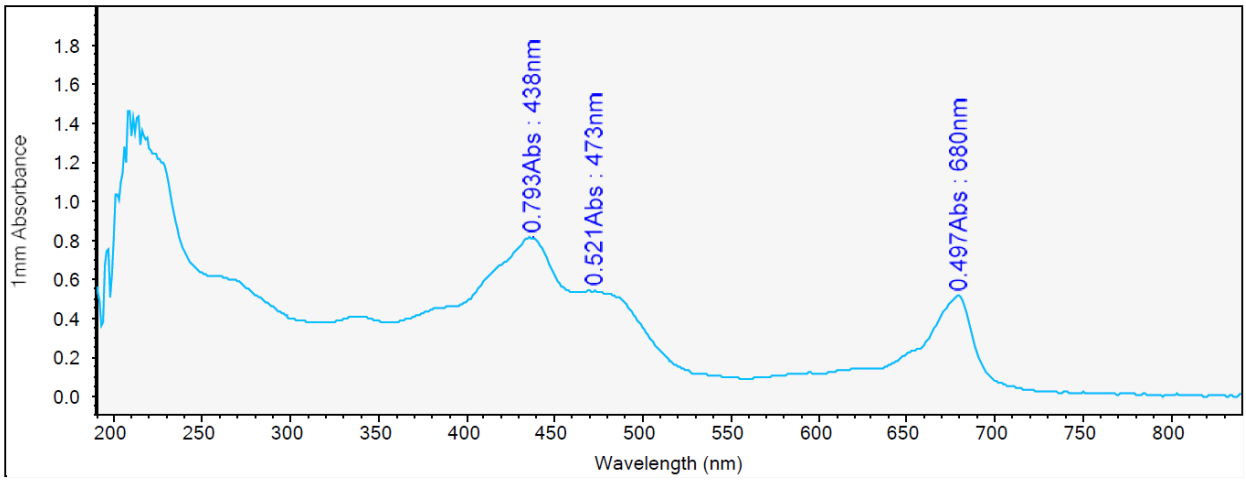

Absorpotion spectrum of thylakoid.

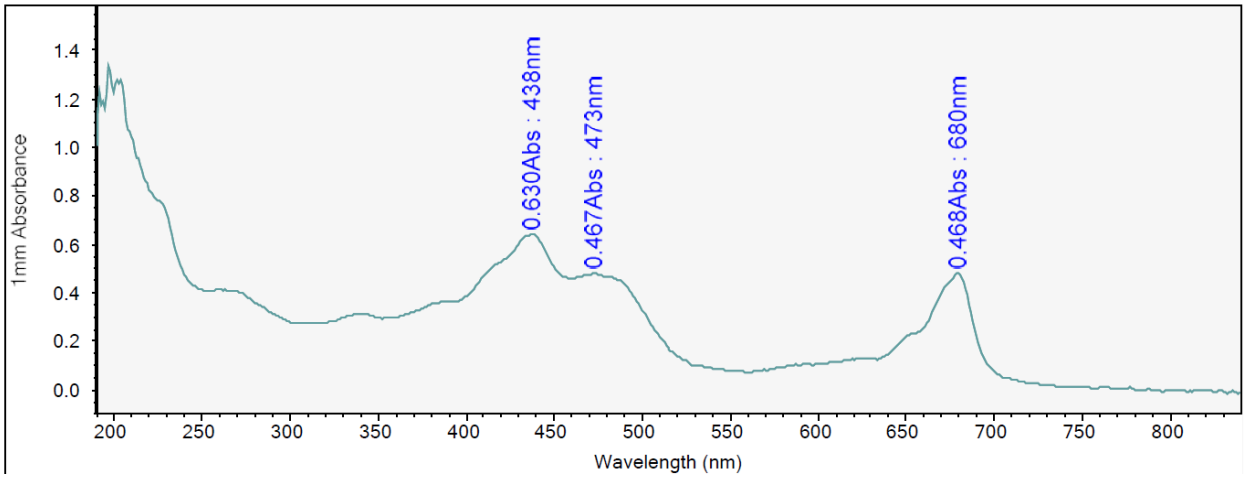

Absorption spectrum of BBY membrane.

4. Image of AuNP suspension.

5. Cyclic voltammogram of AuNP deposition via electropolymerization. Two peaks shown in the figure confirms the successful deposition of AuNP.

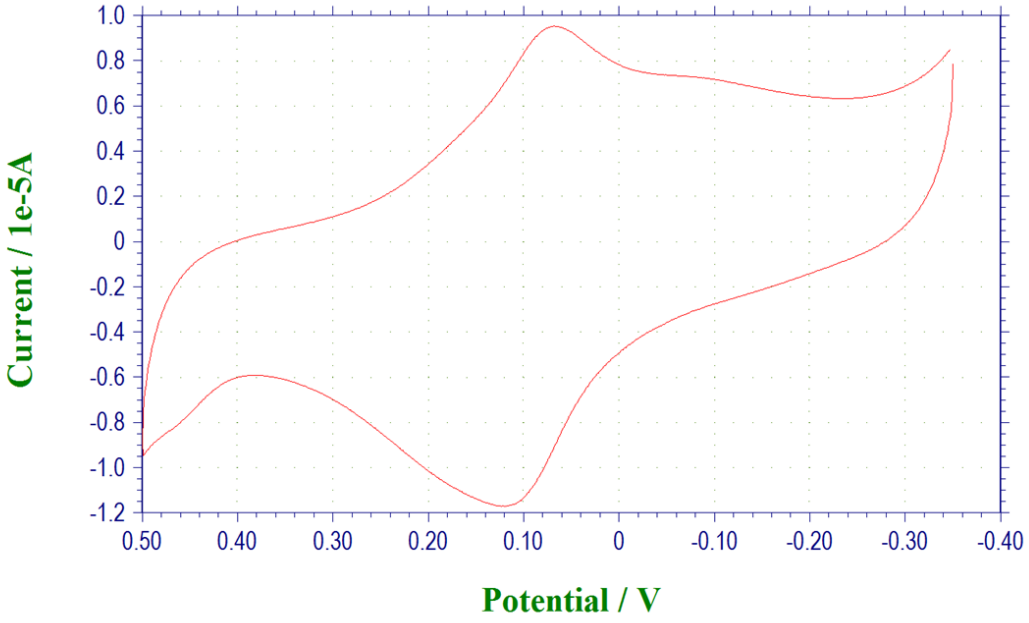

Cyclic voltammogram corresponding to the electropolymerization of the AuNP on the thiol-modified Au coated glass slide. 0.1 M phosphate buffer (pH7.5) was used as the electrolyte. The scan rate is 0.1 V s-1.

6. Protein preparation by using different types of mixing methods.

Table 1. List of samples and various sample preparation methods. Final concentration of chlorophyll was also shown.

#	Mixing	TX-100	Centrifuge Speed (xg)	Final Concentration (mg/ml)
1	Vortex	N	4,600 (for all)	0.538
2	Vortex	Y	4,600 (for all)	0.151
3	Sonication	N	4,600 (for all)	0.185
4	Sonication	Y	4,600 (for all)	0.033
5	Vortex	Y	6,000; 12,000; 50,000	0.709
6	Homogenizer	Y	6,000; 12,000; 50,000	1.859

7. Not working oxygen probe experiment data

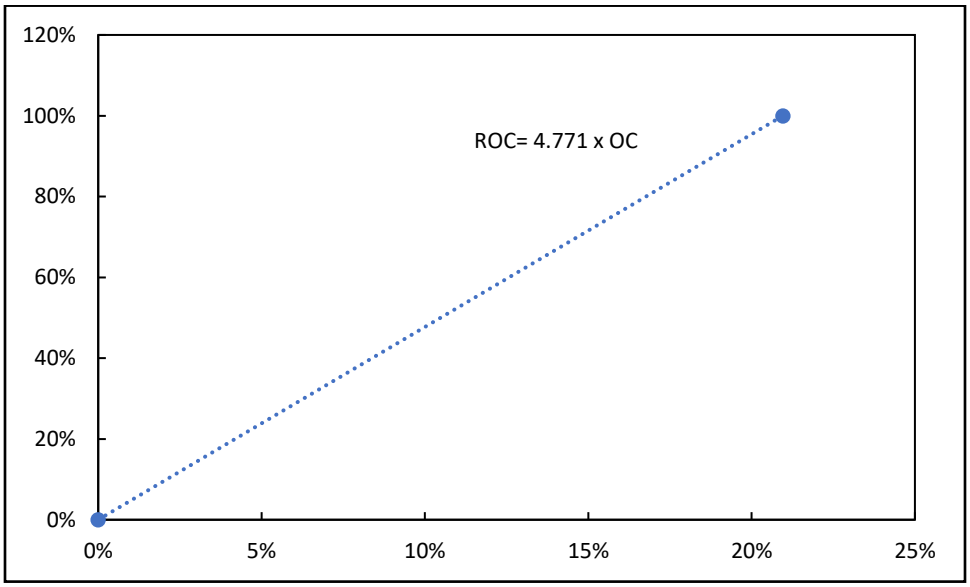

Oxygen probe calibration curve

Where,
ROC: Relative oxygen concentration, %
OC: Oxygen concentration, %

Oxygen evolving experimental data based on the improper working oxygen electrode

5ml Samples	Relative O2%	O2%	O2% Evolving
Vortex + No TX-100	100.3	21.01	1.48
Vortex + TX-100	106.5	22.31	2.78
Sonication + No TX-100	100.2	20.99	1.46
Sonication + TX-100	102.7	21.52	1.99
SMN buffer	93.2	19.53	-
Homogenizing +TX-100	111.93	23.45	3.92

8. Oyxgen probe.

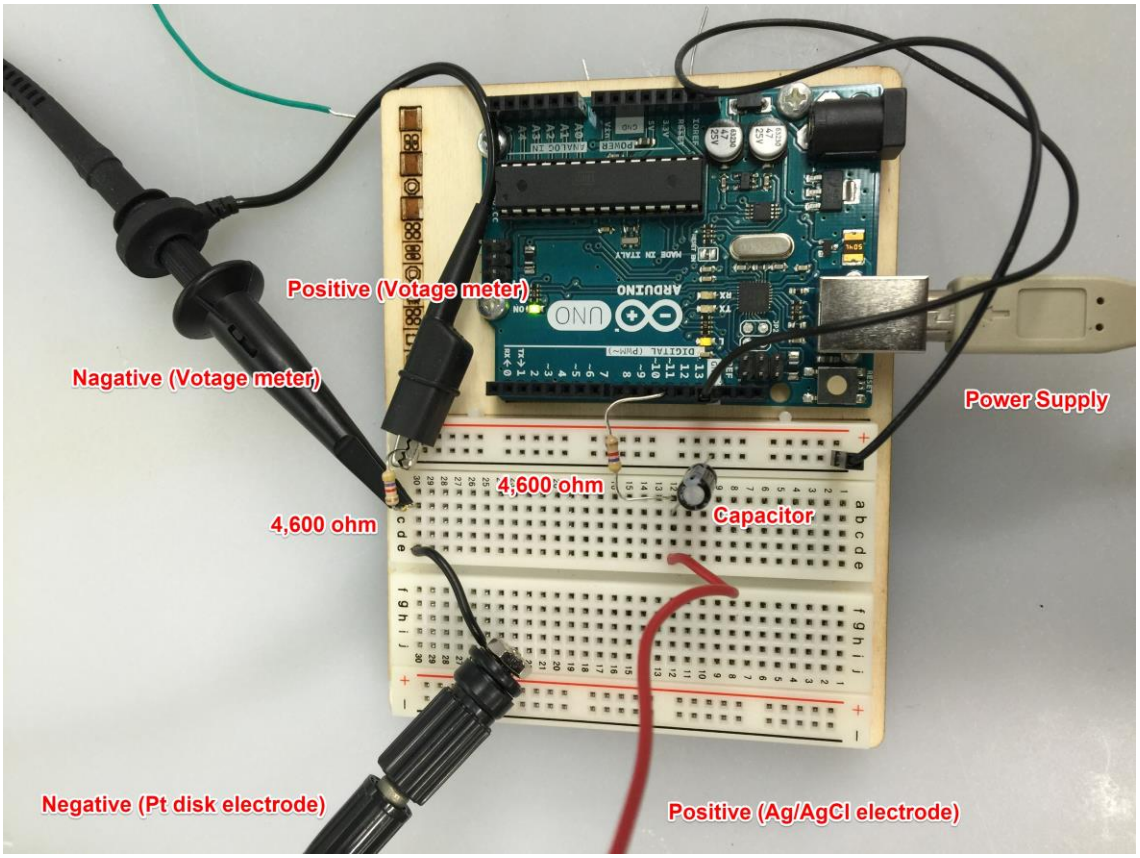

9. Protein gel of obtained BBY membrane

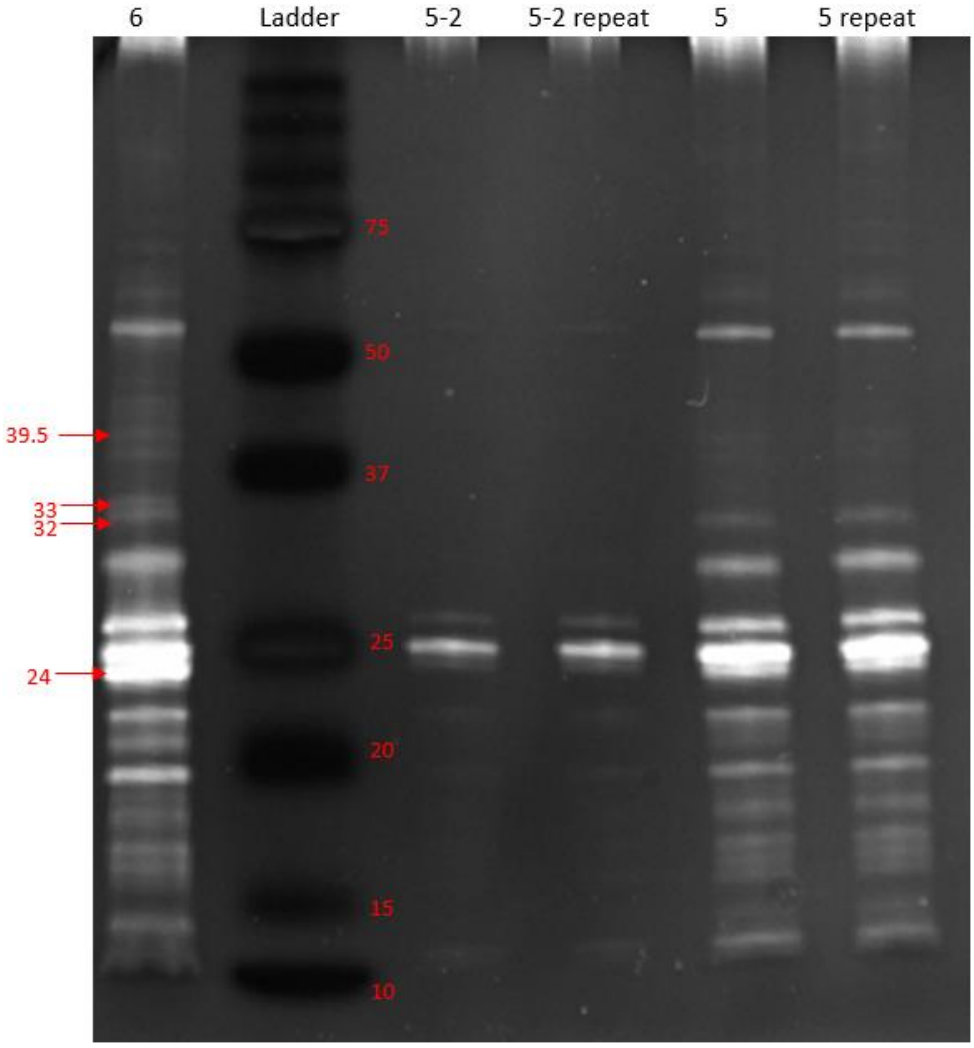

BBY membrane sample #6 consists of all representative proteins. Representative proteins have the protein molecular weight of 24 kDa (peptides), 32 kDa (PsbA), 33 kDa (manganese stability protein), and 39.5 kDa (PsbD). Bands 39.5 kDa and 33kDa are faint in sample #5. Sample #5-2 was prepared from sample #5 by centrifuging #5 at 1,500xg for 1 minute to remove chunks.

Four major proteins within the PSII was needed to be detected in order to confirm the presence of PSII which were peptides, PsbA, PsbD, and the manganese stability protein. As shown in the figure, all four bands could be easily identified in sample #6 and sample #5. Very faited bands were shown in sample #5-2 which might be caused by the low concentration of proteins.

10. Synthesized AuNPs via the Turkevich method.

(a)

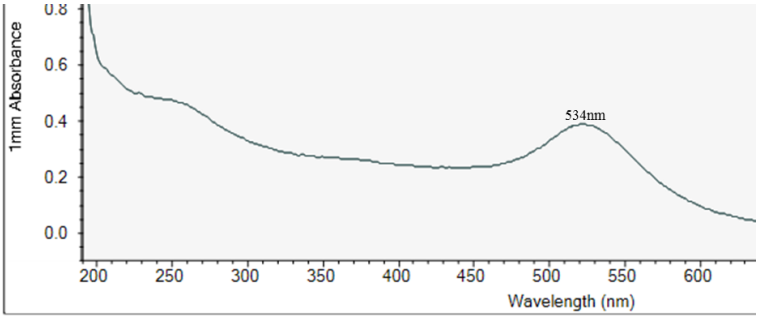

(b)

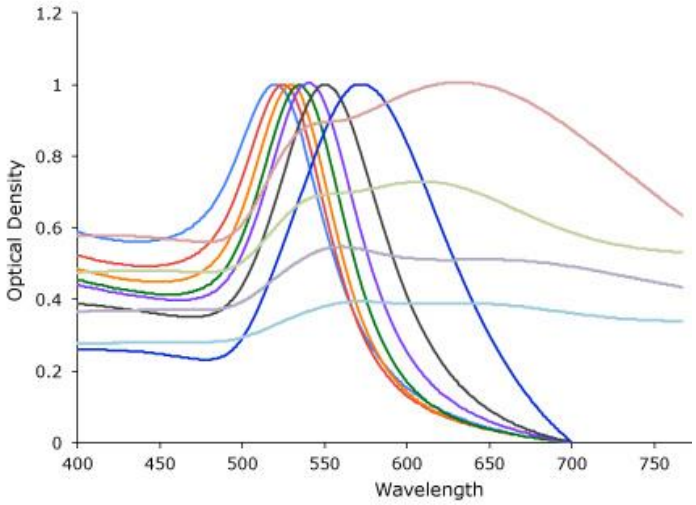

http://www.cytodiagnostics.com/store/pc/Introduction-to-Gold-Nanoparticle-Characterization-d3.htm

(a) The absorbance of an Au NPs solution prepared via the Turkevich method. (b) The spectrum of Au NPs solution with different Au NPs sizes.

11. Approches to use non-modified AuNP during immobilization.

The basic idea of this method is to conduct the electropolymerization before introducing the AuNPs. A p-aminothiophenol modified Au slide was prepared first. Then, 5 mM p-

aminothiophenol solution was prepared in a 0.1 M phosphate buffer (pH 7.5, filtered through a 0.4 um filter disk). Next, the modified Au slide was immersed in the solution and it was electrochemical polymerized via a cyclic voltammetry technique. The scan rate is 50 mV/s in the range of -0.4 to 1.2 V for 30 cycles. Following that, the slide was immediately immersed into a 1 mM AuNPs solution (10 ml, prepared via Turkevich method with a particle size of 19.62 ± 2.99 nm) and 5 mM of mercaptoethane sulfonate (10 ml) was also added into the solution later. The system was reacted for 4 h under 4 °C to introduce Au NPs by self-assembly and modify the AuNP surface with mercaptoethane sulfonate at the same time.

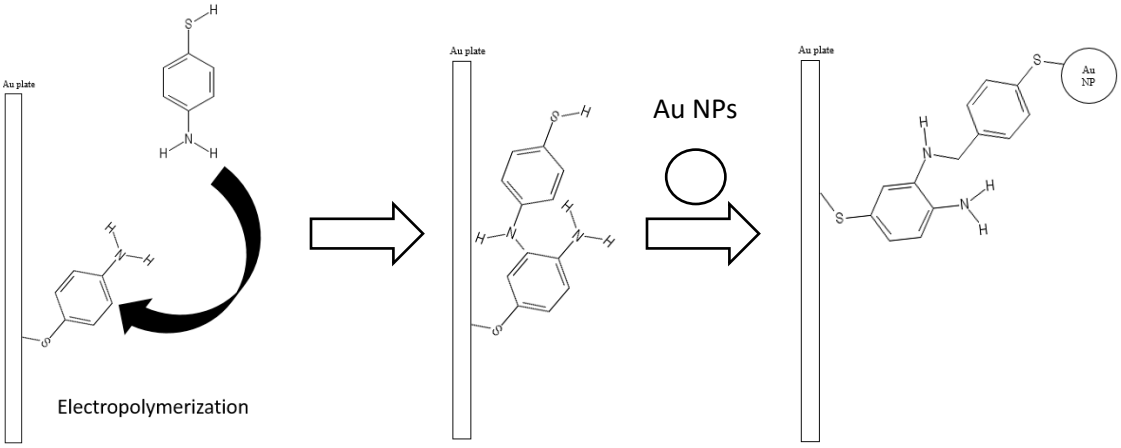

Scheme of the non-modified AuNPs deposition process.

The cyclic voltammogram of electrochemical polymerization is shown in Figure S9. No obvious oxidation or reduction can be observed from the figure. But, after the electropolymerization, white deposits can be seen on the slide.

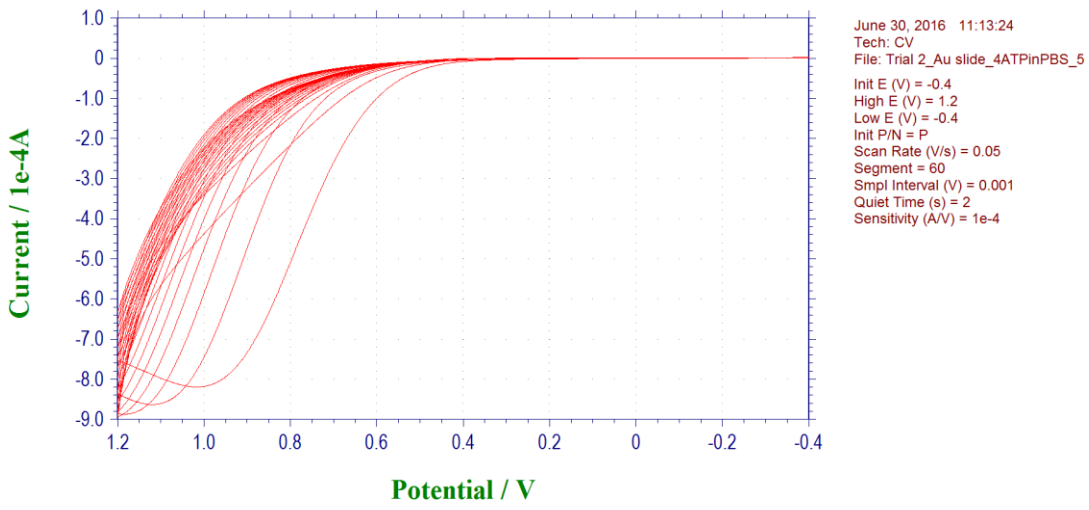

Electropolymerization of p-aminothiophenol onto the p-aminothiopehnol modifield Au slide.

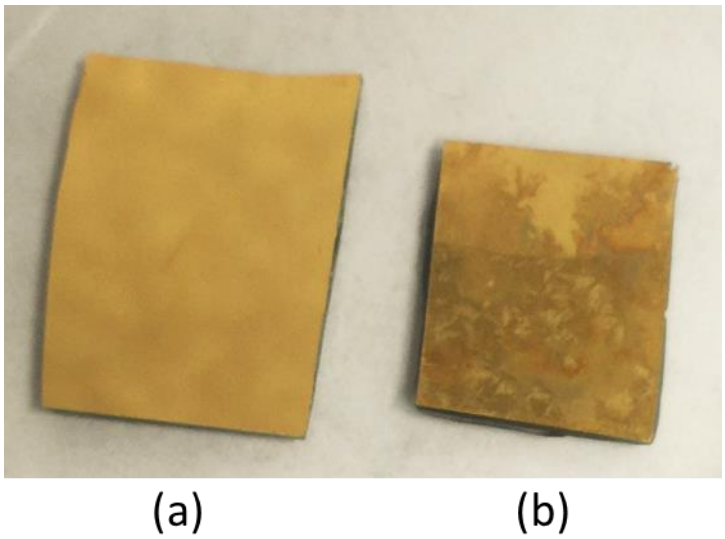

(a) Thiol-modified gold coated glass slide; (b) Thiol-modified gold coated glass slide after conducting electropolymerization in a 5 mM p-aminothiophenol and 0.1 M phosphate buffer, pH 7.5.

12. The proposed current density measurement platform.

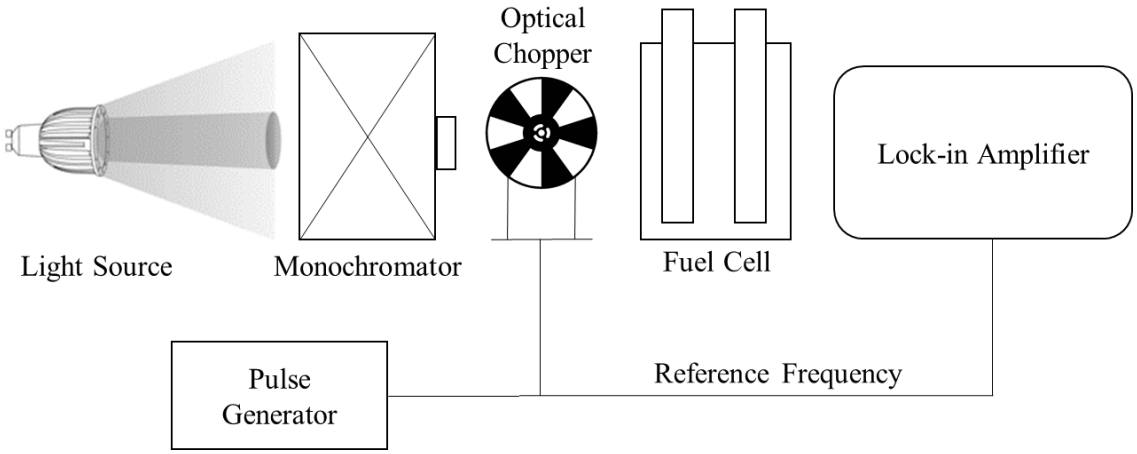

13. SEM images

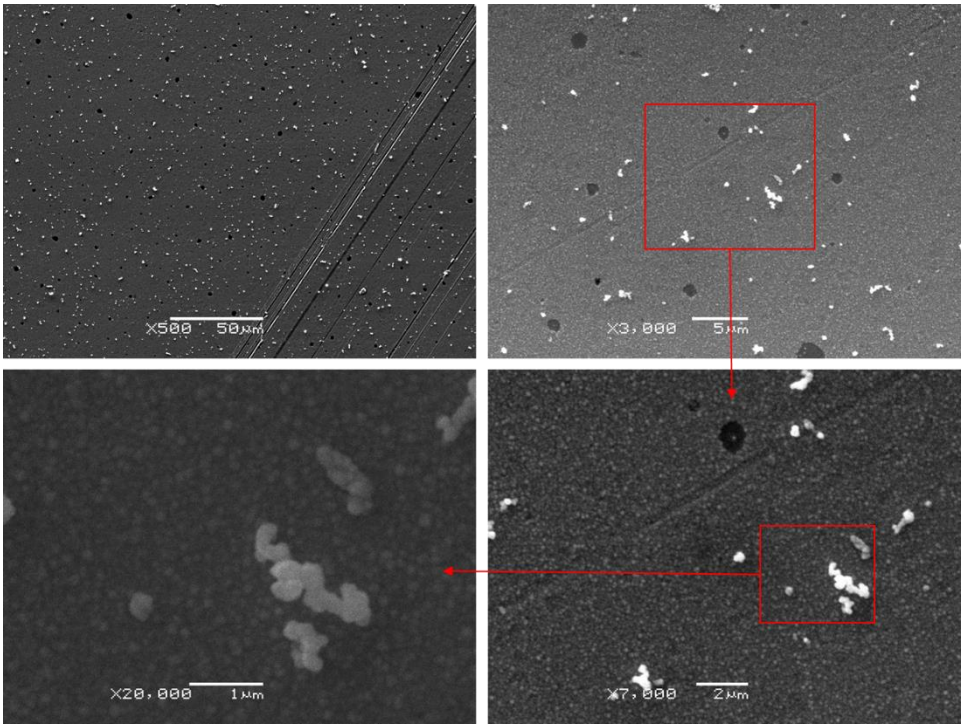

The SEM imge of the Au/AuNP construction was shown with different magnitudes. Successful deposition of AuNP was observed.

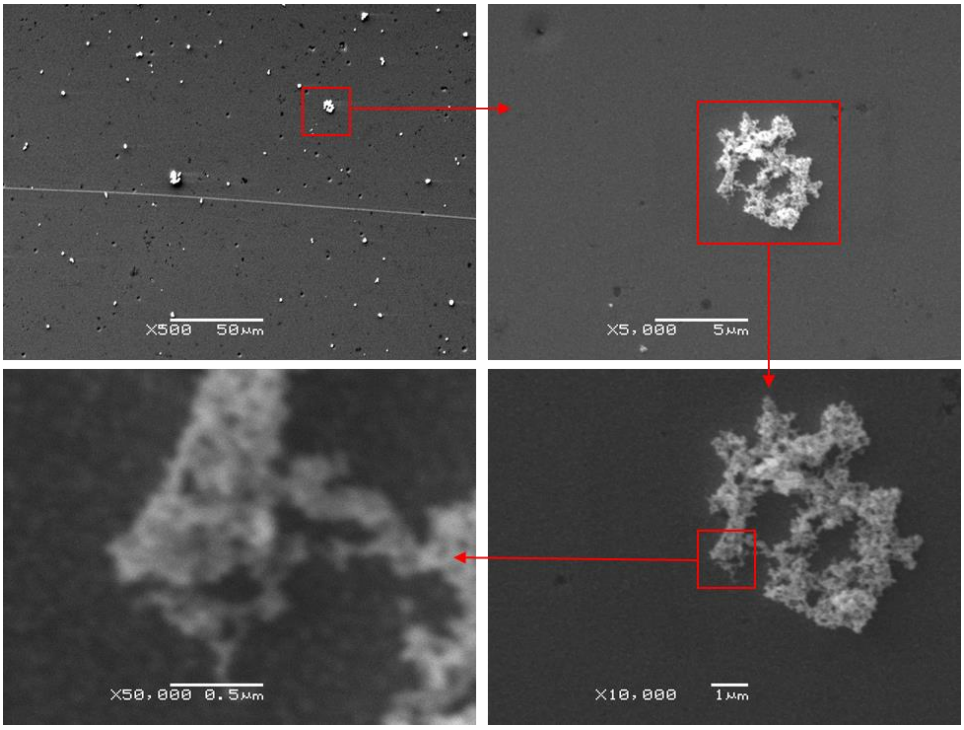

The SEM image of the Au/AuNP/BBY system. A possible protein structure was observed in the image.

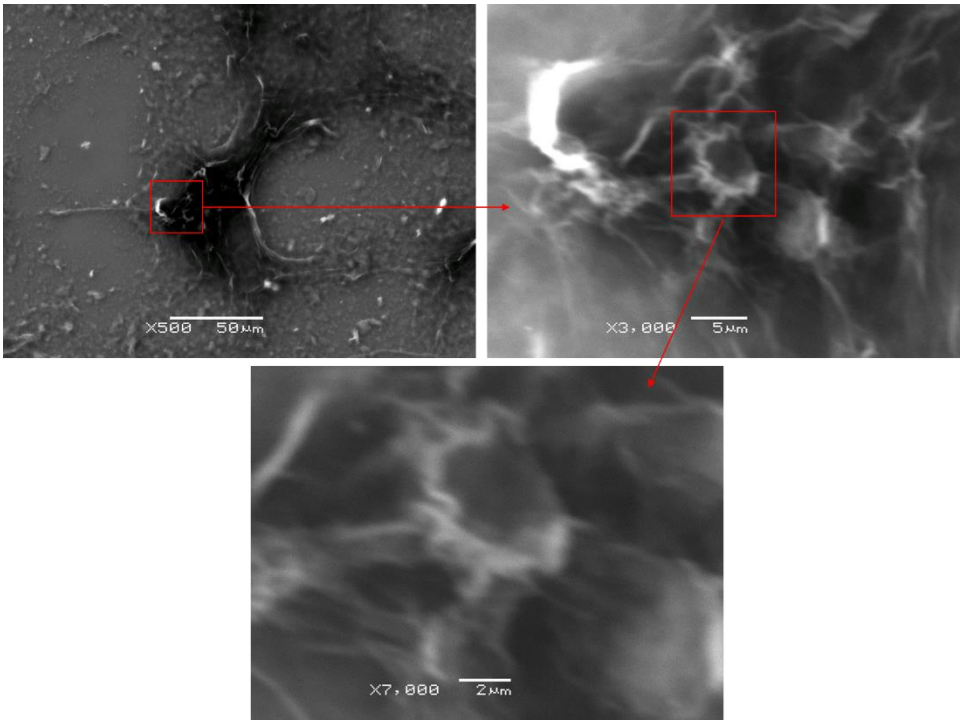

The SEM image of the ITO/MWCNT construction. Possible MWCNT was observed in the image.

14. Electrodeposition of the MWCNT onto the ITO slide

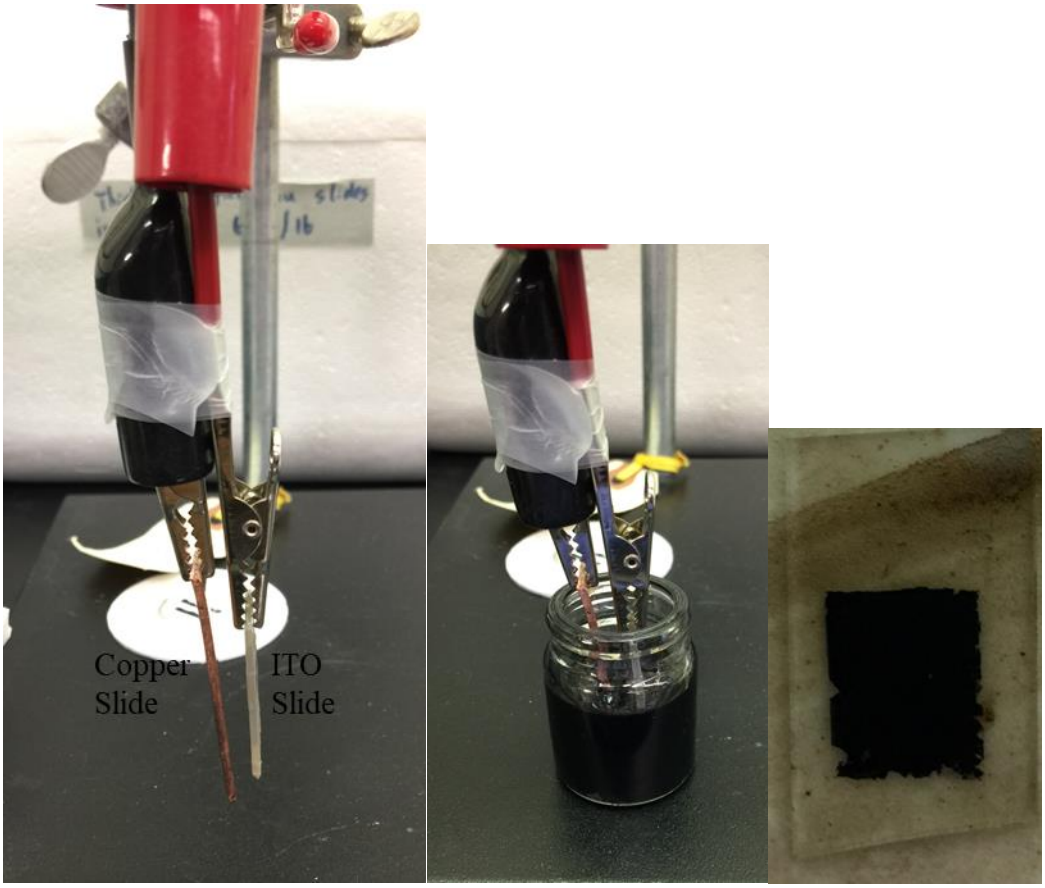

15. Delayed current response to the light on/off test.

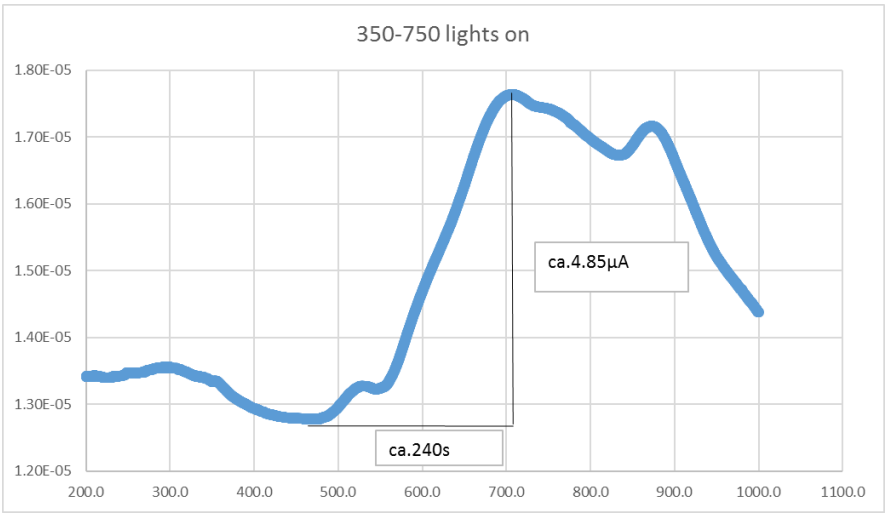

i-t graph of sample ITO/MWCNT/BBY. -0.3 V voltage applied. Light on at 350-750s.